Available online at www.sciencedirect.com
SCIENCE DIRECT®
ELSEVIER
European Journal of Mechanics B/Fluids 22 (2003) 331–343
EUROPEAN JOURNAL OF MECHANICS B/FLUIDS

Flow of magnetorheological fluid through porous media

Pavel Kuzhir [a], Georges Bossis [b,*], Victor Bashtovoi [a], Olga Volkova [b]

[a] *UNESCO chair "Energy Conservation and Renewable Energies", Belarusian National Technical University, 65, F. Skaryna Ave., Minsk 220013, Belarus*
[b] *Laboratoire de physique de la matière condensée, Université de Nice-Sophia Antipolis, CNRS, UMR 6622, UNSA, Parc Valrose 06108, Nice cedex 2, France*

Received 26 February 2003; received in revised form 6 May 2003; accepted 12 May 2003

Abstract

Flow of a magneto-rheological (MR) fluid through different types of porous media (bundle of cylinders, packed beds of magnetic and non-magnetic spheres and cylinders) is considered, both theoretically and experimentally. The theory is based on averaging the magnetic and rheological properties of MR fluid in tortuous channels making different angles between local field and local velocity. A comparison of the pressure drop through porous beds and spiral channels is analyzed and practical recommendations are developed. It is shown that the mean yield stress of Bingham MR fluid (as well as the pressure drop, ΔP) depends on the mutual orientation of the external magnetic field and the main axis of the flow. This theory is tested against our experimental results and is shown to well predict the pressure drop obtained in different porous media.

Keywords: Magnetorheology; Magnetic suspensions; Active damping; Bingham fluid; Porous media

Notation

$\mathbf{B}$	magnetic field induction
D	diameter of porous column
d	diameter of granular particles
e	eccentricity of an ellipsoid of revolution
$\mathrm{f}(\theta)$	frequency distribution function of the channel orientation
$f_\mathrm{d} = \langle H_\mathrm{f} \rangle / H_0$	factor characterizing demagnetization effect in porous sample
$\mathbf{H}$, H	magnetic field intensity
$\mathbf{H}_0$, H_0	intensity of the external uniform magnetic field
L	length of the cylindrical porous column
l	length of ellipsoidal or cylindrical granular particle
Mn	Mason number
$\mathbf{N}$ (N)	tensor (value) of demagnetization factors
P (ΔP)	pressure (pressure drop)
Q	volume flow rate
R_e	equivalent radius of pores
V	volume
v	velocity of MR fluid in a tortuous channel

* Corresponding author.
E-mail addresses: kuzhir@biobel.bas-net.by (P. Kuzhir), bossis@unice.fr (G. Bossis).

0997-7546/$ – see front matter
doi:10.1016/S0997-7546(03)00040-2

v_0 superficial velocity
$x,\ y,\ z$ coordinates of the Cartesian system

Greek letters

α angle between the main axis of the flow and the direction of the mean field $\langle \mathbf{H} \rangle$ in a porous medium
$\dot{\gamma}_w$ wall shear rate
ε porosity
$\phi,\ \theta$ angles of spherical coordinate system
η_p plastic viscosity
μ relative magnetic permeability
μ_0 magnetic permeability of vacuum
τ_B Bingham yield stress
τ_{B0} Bingham yield stress in the magnetic field perpendicular to the flow
τ_w wall shear stress
ξ tortuosity
ψ angle between the local flow and magnetic field in a porous medium

Subscripts

f liquid phase of a porous medium
s solid phase of a porous medium

Superscripts

$*$ normalized values

1. Introduction

Magneto-rheological (MR) fluids are used to control, by the mean of a magnetic field, the flow rate or the pressure drop inside hydraulic devices. A key problem for practical use is to find the best design of the channels where the magnetic fluid will flow. This poses the problem of the orientation of the field relatively to the velocity. It is possible to demonstrate that, for a pressure driven flow inside a straight channel, the best configuration is the one where the field is perpendicular to the velocity. This configuration can be obtained by using a spiral channel inside a coil. An other simple device could be obtained with the tortuous channels that naturally exist in porous media. Flow of MR fluids through packed beds of non-magnetic spheres filling a solenoid has been investigated by Shulman et al. [1,2]. From their measurements they conclude that porous beds were more efficient than spiral channels. Actually at the scale of the pore size (micro-scale), the flow is not unidirectional, and the local field has various orientations relatively to the velocity of MR fluid. Furthermore, high local non-uniformity of the magnetic field can take place, especially if we use a magnetic porous media, because of demagnetization effect in irregular porous matrix. At the micro-scale local values of the magnetic field depend on the configuration and size of pores. At scale of the whole porous matrix (macro-scale), mean values of the field depend on magnetic properties and configuration of the porous matrix, so both scales are important to model the behavior of a MR fluid in a porous media.

In the second section of this paper we have presented the experimental device and materials we have used for investigation of the flow of MR fluid through a porous medium. In the third part we have described the experimental results we have obtained for different kinds of porous media. The section four is devoted to the presentation of the model we have used to predict the discharge curve (a volume flow rate versus pressure gradient dependence) for different magnetic fields and any kind of porous media (made of spheres or cylinders of different aspects ratio and also made of magnetic or non-magnetic materials); a comparison between theoretical predictions and experimental results is also presented in this section.

2. Experimental device and materials

For the investigation of MR fluid flow through porous media in magnetic field parallel to the flow, the following experimental setup has been used Fig. 1(a). The hydraulic loop consists of a double-acting piston filled with hydraulic oil, two rubber membranes, and two solenoids surrounding a core filled by MR fluid and connected by a plastic tube. The membranes separate MR fluid from oil and transmit motion from the piston to MR fluid. The use of two different fluids prevents a possible damage of the piston caused by MR fluid abrasive particles. The porous samples having the shape of a cylindrical column were placed in a tube at the center of the solenoids in the region of uniform magnetic field. While filling with MR fluid, degassing of the system was performed with a vacuum pump. The pressure was measured as the piston moved from one extremity to the other with a given constant velocity independent of the hydraulic resistance of the hydraulic loop. Then the piston returned to its initial position. The pressure difference over the working section is up to 2 MPa and measured by two pressure transducers. The flow rate (up to $6 \times 10^{-6}\ \mathrm{m}^3 \cdot \mathrm{s}^{-1}$) was controlled by an electric drive of the piston.

We have used a brushless electric motor SBC Electronica SPA NB707001, a frequency converter SBC Electronica SPA HPD2N, that drives the motor, a frequency converter RS-422/RS-485 for linking HPD2N-converter with a PC acquisition card Intelligent Instrumentation PCI-20428W. Electric current in the solenoids reached 8 A corresponding to the magnetic field intensity $H = 64\ \mathrm{kA} \cdot \mathrm{m}^{-1}$.

Two kinds of porous samples have been used, namely isotropic and anisotropic ones. Anisotropic media are made of packed bundles of long non-magnetic cylinders of two sizes, placed parallel to the solenoid axis (Fig. 1(b)-(1)). Isotropic samples are either packed beds of non-magnetic or magnetic spheres (Fig. 1(b)-(2)) or also randomly oriented non-magnetic cylinders (Fig. 1(b)-(3)). Magnetic spheres used are made from magnetically soft bulk steel with the field dependence of relative permeability given by Frolisch–Kennelly law:

$$\mu^{\mathrm{b,s}}(H) = 1 + \frac{(\mu_{\mathrm{i}} - 1)M_{\mathrm{s}}}{M_{\mathrm{s}} + (\mu_{\mathrm{i}} - 1)H}, \tag{1}$$

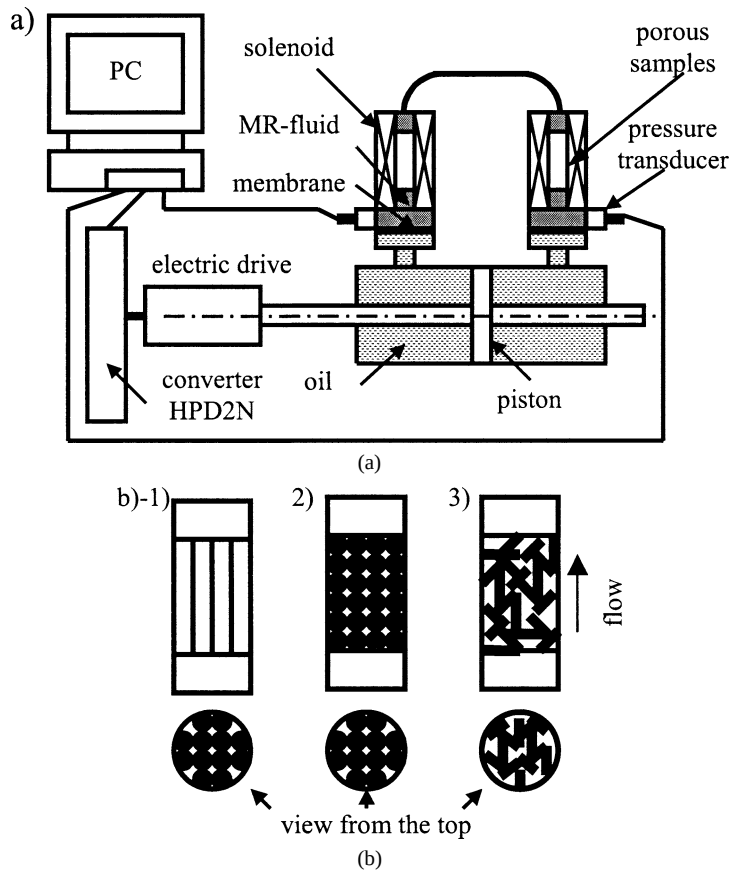

Fig. 1. (a) Experimental setup; (b) Different kinds of porous beds.

where $\mu_i = 250$ is the initial magnetic permeability, $M_s = 1360\ \mathrm{kA \cdot m^{-1}}$ is the saturation magnetization.

Following the Kozeny–Carman model [3] of porous medium (model of tortuous channels), the latter is characterized by porosity, ε, tortuosity, ξ, and equivalent radius R_e of pores. The porosity of a bundle of N cylinders is given by the formula $\varepsilon = 1 - Nd^2 l/(D^2 L)$. Hereafter, d, l stand respectively for the diameter and length of cylinders and D, L do for the dimensions of the cylindrical porous bed. Porosity of beds was determined by the gravimetric method. The tortuosity $\xi \geqslant 1$ is the ratio of the length of a tortuous channel of a porous sample to the length of the sample. For a bundle of cylinders the tortuosity is unity ($\xi = 1$) by definition; for packed beds it was determined from the pressure measurements of the flow of two standard fluids (silicon oil of viscosity 0.1 and 1 Pa · s) as well as of MR fluid in the absence of field. For each of these three fluids we have obtained the same result on ξ.

The equivalent radius R_e of pores is defined as the radius of the cylindrical channel having the volume equal to the volume V_f of the liquid phase of the porous medium and the surface equal to the total wetted surface S_s of the solid phase: $R_e = 2V_f/S_s = 2(V_p/S_p) \cdot (\varepsilon/(1-\varepsilon))$ with V_p and S_p being the volume and surface of particles. This definition follows from the capillary model of porous media [4]; for a cylindrical capillary R_e is the radius of the capillary. Some authors utilize the "hydraulic radius" R_h, which is connected with the equivalent radius through the expression $R_h = R_e/2$ [3]. The following formulas are used for R_e: $R_e = d\varepsilon/(2(1-\varepsilon))$ for the bundle of cylinders, $R_e = d\varepsilon/(3(1-\varepsilon))$ for the bed of spheres and $R_e = d\varepsilon/[(2 + d/l)(1-\varepsilon)]$ for the bed of cylinders. All characteristics and dimensions of porous matrixes are presented in Table 1.

In experiments we have used a MR fluid made of OTE carbonyl iron particles supplied by BASF, dispersed in silicon oil 47V20 and stabilized by a silicagel Aerosil-300, the volume fraction of magnetic particles is 30%. MR fluid has a density $\rho = 3000\ \mathrm{kg \cdot m^{-3}}$, a relative magnetic permeability: $\mu_f = 4.8$ in structured media and $\mu_f = 2.5$ in non-structured one, a yield stress $\tau_{Bi} = 25$ Pa and plastic viscosity $\eta_{pi} = 0.14$ Pa · s, both in the absence of field. Rheological properties in the presence of the magnetic field transverse to the shear flow were measured in cone-plane geometry with a rheometer Haake RS-150. In the range $200 < \dot{\gamma} < 1500\ \mathrm{s^{-1}}$ and for fields $0 < H < 15\ \mathrm{kA \cdot m^{-1}}$, we observed a Bingham behavior with the yield stress following the empirical law:

$$\tau_{B0} = 10\mu_0 H^2, \tag{2}$$

where μ_0 is the permeability of vacuum.

The plastic viscosity η_p remains practically constant within the field range considered. At low shear rates (below $100\ \mathrm{s^{-1}}$), flow curves are no longer linear and indicate that the real yield stress can be significantly lower than the one given by Eq. (2), which was obtained by the linear interpolation of a flow curve to zero shear rate. In any event, in the range of shear rates that we use, Eq. (2) well represents the rheological behavior of our fluid.

For a given external magnetic field, $\mathbf{H}_0$, the field $\mathbf{H}_f$ inside MR fluid for the bundle of long cylinders is supposed to be undisturbed and equal to the external one. For porous beds, the mean field in MR fluid $\langle \mathbf{H}_f \rangle$ will be determined as specified in Section 4.1.

Table 1
Characteristics of the porous samples used in experiments

No of sample	1	2	3	4	5	6	7
Type of sample	bundle of cylinders	bundle of cylinders	bed of spheres	bed of spheres	bed of spheres	bed of spheres	bed of cylinders
Material	inox. steel	inox. steel	$A1_2O_3$-ZrO_2	silica glass	bulk steel	bulk steel	inox. steel
Dimension of grains, mm	∅2 × 70	∅1 × 70	∅1.4	∅0.9	∅2	∅1	∅1 × 5
Dimension of sample, mm	∅10 × 70	∅10 × 70	∅10 × 70	∅7.5 × 20	∅10 × 70	∅7.5 × 20	∅10 × 70
Porosity ε	0.24	0.25	0.40	0.42	0.42	0.41	0.48
Tortuosity ξ	1	1	1.45	1.44	1.41	1.44	1.63
Equivalent radius, R_e, mm	0.41	0.26	0.31	0.22	0.48	0.23	0.52
Internal-to-external field ratio $\langle H_f \rangle / H_0$ at $H_0 = 20\ \mathrm{kA \cdot m^{-1}}$	1	1	0.87	0.87	1.45	1.55	0.89
Fit coefficients of $\tau^* = C \cdot \mathrm{Mn}^{-n}$:							
n	0.92	0.94	0.93	0.90	0.92	0.89	0.96
C	4.90	6.12	16.9	25.2	21.2	19.9	33.3

3. Experimental results

In porous media, the discharge curves are usually presented as the dependence of the pressure drop ΔP (or the pressure gradient value $\Delta P/L$) on the superficial velocity v_0. The latter is the ratio of the flow rate Q to the porous sample cross-section and is connected with the mean velocity v in a tortuous channel through the relation $v_0 = v\varepsilon/\xi$. Discharge curves for different types of porous samples and with different values of the external magnetic field H_0 are shown in Fig. 2. All the discharge curves including those not shown in Fig. 2 are linear and correspond to wall shear rate up to 10^4 s^{-1} inside the porous channels. The extrapolation of these curves to the axis $v_0 = 0$ gives the yield pressure gradient $(\Delta P/L)_{v=0}$. This value is the apparent threshold where the MR fluid begins to flow. As already pointed, the real yield stress is smaller than the one obtained from this extrapolation, which corresponds to the dynamic yield stress of a Bingham model. Therefore true value of the initial pressure gradient should also be lower than the apparent one.

Comparing Fig. 2(b) for porous bed of nonmagnetic spheres to Fig. 2(c) corresponding to magnetic spheres of nearly the same diameter, we see that the magnetic bed gives a much higher pressure drop for a same external magnetic field. We shall see in the following Section 4.1 that this result is due to the fact that the mean magnetic field $\langle \mathbf{H}_f \rangle$ in MR fluid is higher for a magnetic porous matrix than for a nonmagnetic one, due to different demagnetization effects. Therefore for the same external field, the mean yield stress as well as the pressure gradient are higher for the magnetic porous media. The pore radius R_e of the bed of non-magnetic cylinders is more than 2 times larger than that of non-magnetic spheres, therefore the pressure gradient is higher for spheres, for a same magnetic field, as can be seen by comparing Figs. 2(b) and 2(d). At least we see in Fig. 2(a), that a bundle of cylinders gives the lowest pressure gradient as we could expect, since in this case we have straight channels with the field aligned on the velocity.

We wish now to determine a rheological law for MR fluid flow in a porous medium. According to [3], the rheological behavior of non-Newtonian fluids in porous media can be characterized by quantities, like wall shear stress τ_w and wall shear rate $\dot{\gamma}_w$:

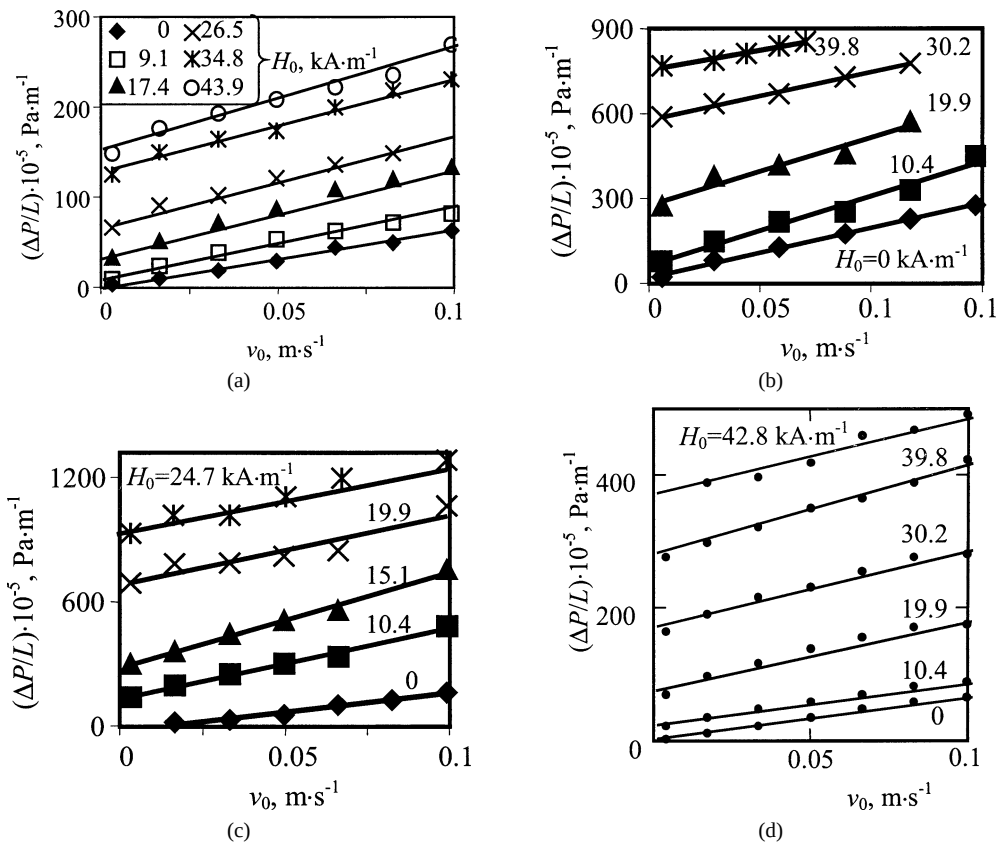

Fig. 2. Dependence of the pressure gradient value on the superficial velocity for the following porous samples: (a) bundle of cylinders ∅1 mm, (b) bed of non-magnetic spheres ∅ 0.9 mm; (c) bed of magnetic spheres ∅1 mm, (d) bed of non-magnetic cylinders: ∅1 mm, length 5 mm.

$$\tau_{\mathrm{w}} = \frac{\Delta P R_{\mathrm{e}}}{2\xi L}, \tag{3}$$

$$\dot{\gamma}_{\mathrm{w}} = \frac{4\nu_0 \xi}{\varepsilon R_{\mathrm{e}}}. \tag{4}$$

The last expression is the apparent wall shear rate $\dot{\gamma}_{\mathrm{w}}$, calculated for a Newtonian fluid. For other fluids the true value of wall shear rate is determined by Mooney–Rabinowitch procedure [1]. In a previous work [5], we have defined the rheological behavior of MR fluid in a single cylindrical capillary subjected to an inclined magnetic field. At high shear rates, we have found a Bingham behavior:

$$\tau_{\mathrm{w}} = \frac{8}{3\pi}\tau_{\mathrm{B}} + \eta_p \dot{\gamma}_w, \tag{5}$$

with a yield stress $\tau_{\mathrm{B}} = (\tau_{\mathrm{B1}} + \tau_{\mathrm{B2}})/2$ (in fact, there are two yield stresses τ_{B1} and τ_{B2}, which correspond to zones of positive and negative velocity gradient: see [5] for details) and plastic viscosity η_{p}. The factor $8/(3\pi)$ in front of τ_{B} in Eq. (5) differs from unity because we deal with apparent wall shear rate $\dot{\gamma}_{\mathrm{w}}$ and because of the anisotropy of the plug [5]. So, for a system of tortuous channels, we expect that the rheological law will have the same form as (5) with $\langle\tau_{\mathrm{B}}\rangle$ averaged over the different orientations between field and flow. Substituting the expressions (3), (4) for τ_{w} and $\dot{\gamma}_{\mathrm{w}}$ into Eq. (5), we obtain the pressure gradient vs. velocity dependence:

$$\frac{\Delta P}{L} = \frac{16\xi}{3\pi} \cdot \frac{\langle\tau_{\mathrm{B}}\rangle}{R_{\mathrm{e}}} + \frac{8\langle\eta_{\mathrm{p}}\rangle\xi^2}{\varepsilon R_{\mathrm{e}}^2}\nu_0. \tag{6}$$

Using this formula, unknown values of the mean yield stress and mean plastic viscosity can be obtained from the fit of experimental discharge curves shown in Fig. 2. Dependencies of these quantities on the magnetic field $\langle H_{\mathrm{f}}\rangle$ in MR fluid are shown in Fig. 3 for various porous samples. It appears that all experimental points $\langle\tau_{\mathrm{B}}\rangle(\langle H_{\mathrm{f}}\rangle)$ are grouped into two series of points represented by the two solid lines in Fig. 3(a). The lower curve corresponds to results on porous samples made of straight channels, the upper curve corresponds to results on packed beds. As expected, the yield stress for packed beds is far larger than for straight channels. It comes from the change of relative orientation of the flow with respect to the one of the magnetic field in tortuous channels of packed beds, so that the average yield stress $\langle\tau_{\mathrm{B}}\rangle$ is higher than in the case where the field and the flow are aligned. Within the whole range of magnetic fields (up to 50 kA/m), the plastic viscosity has a constant value: $\langle\eta_{\mathrm{p}}\rangle = 0.16 \pm 0.03$ Pa · s, that is close to its value $\eta_{\mathrm{pi}} = 0.14$ Pa · s in the absence of field (Fig. 3(b)).

Finally, we present all the discharge curves in normalized form $\tau^* = \mathrm{f(Mn)}$. Here $\tau^* = (\tau_w - \tau_{Bi})/(\eta_{pi}\dot{\gamma}_w) - \eta_p/\eta_{pi}$ is the normalized stress, $\mathrm{Mn} = (8\eta_{pi}\dot{\gamma}_w)/(\mu_0\langle H_f\rangle^2)$ is the Mason number, which characterizes the ratio of hydrodynamic to magnetic forces. Similarly to the field dependence of the yield stress, normalized flow curves $\tau^* = \mathrm{f(Mn)}$ for packed beds and for straight channels form two separate groups (Fig. 4). All the curves are approximated by the dependence $\tau^* = C \cdot \mathrm{Mn}^{-n}$. Experimental values of coefficients C and n are presented in Table 1. Slopes n of each curve are close to the unity, that corresponds to Bingham behavior.

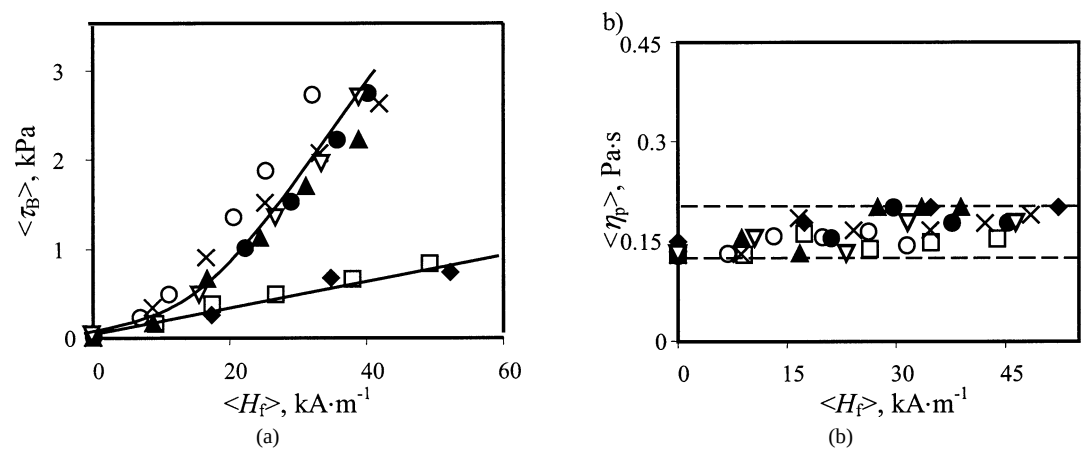

Fig. 3. Dependencies of the mean Bingham yield stress (a) and the mean plastic viscosity (b) on the magnitude of the internal magnetic field $\langle H_{\mathrm{f}}\rangle$ for different porous samples: bundle of cylinders, ∅ mm: ♦ 2, □ 1; bed of non-magnetic spheres ∅ mm: ▲ 1.4, × 0.9; bed of magnetic spheres ∅ mm: ● 2, ▽ 1; bed of cylindrical particles ○ ∅1 × 5 mm.

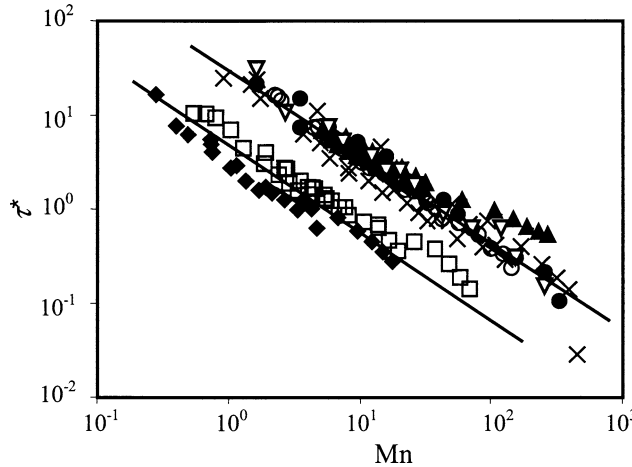

Fig. 4. Normalized stress versus Mason number in porous media (Notations are the same as in Fig. 3.)

4. Theory

The average yield stress $\langle\tau_B\rangle$ has been obtained from the experiments, through a fit of Eq. (6), as a function of magnetic field intensity and porous media characteristics. Now we are going to see how we can predict this average yield stress.

4.1. Magnetic field $\langle H_f\rangle$ inside the MR fluid

First, we need to average the magnetic field in the volume of a porous medium filled with MR fluid. We are in the case where the dimension of pores is much smaller than the one of the whole porous sample, but much larger than the diameter of MR fluid magnetic particles. Thus, at scale of pore dimension, MR fluid can be considered as an homogeneously magnetized medium. The porous medium is therefore a two-phase disperse system containing liquid phase (MR fluid with relative magnetic permeability μ_f) and solid phase (particles making the porous bed with permeability μ_s).

While averaging, we use three mean values of the magnetic field intensity, namely, the field $\langle\mathbf{H}\rangle$ averaged over the whole volume V of the porous medium, the field $\langle\mathbf{H}_f\rangle$ in the liquid phase averaged over the volume V_f of the liquid phase and the field $\langle\mathbf{H}_s\rangle$ in the solid phase averaged over the volume V_s of the solid phase. These values are connected with each other through the following relationship

$$\langle\mathbf{H}\rangle = \varepsilon\langle\mathbf{H}_f\rangle + (1-\varepsilon)\langle\mathbf{H}_s\rangle. \tag{7}$$

According to [6], the magnetic field $\langle\mathbf{H}\rangle$ in a porous medium is determined in the same way as for a continuous medium, i.e., using Maxwell equations. In the general case of a porous sample of arbitrary shape subjected to uniform external field $\mathbf{H}_0$, the field $\langle\mathbf{H}\rangle$ is non-uniform at the scale of sample dimension. But it is assumed to be uniform at the scale of a pore. If the porous sample has a regular shape, in our case a cylindrical column, the magnetic field $\langle\mathbf{H}\rangle$ can be considered as uniform, and is related to the external uniform field $\mathbf{H}_0$ through the tensor $\mathbf{N}^p$ of demagnetization factors of the porous sample [7]:

$$\langle\mathbf{H}\rangle + \big(\langle\mu\rangle - 1\big)\mathbf{N}^p\cdot\langle\mathbf{H}\rangle = \mathbf{H}_0, \tag{8}$$

where $\langle\mu\rangle$ is the effective relative magnetic permeability of the porous bed. For composite isotropic materials, the effective magnetic permeability is $\langle\mu\rangle = \langle\mathbf{B}\rangle/\langle\mathbf{H}\rangle$ by definition [7]. So, to calculate $\langle\mu\rangle$, we have to average the magnetic field induction $\mathbf{B}$ over the volume V of the porous sample. Following Landau–Lifchitz [7], we use the identical relation $\langle\mathbf{B}\rangle - \mu_f\langle\mathbf{H}\rangle \equiv \frac{1}{V}\int_V(\mathbf{B}-\mu_f\mathbf{H})\,dV$. The integral is calculated separately over the volumes V_s and V_f of solid and liquid phases

$$\frac{1}{V}\int_V(\mathbf{B}-\mu_f\mathbf{H})\,dV = \frac{1}{V}\int_{V_f}(\mathbf{B}-\mu_f\mathbf{H})\,dV + \frac{1}{V}\int_{V_s}(\mathbf{B}-\mu_f\mathbf{H})\,dV$$

with $\mathbf{B}=\mu_f\mathbf{H}$ in the liquid phase and $\mathbf{B}=\mu_s\mathbf{H}$ in solid phase. We suppose that the permeabilities μ_f and μ_s are field independent. So, the integral over the volume V_f is zero and the one over V_s gives

$$\frac{1}{V}\int_{V_s}(\mathbf{B}-\mu_f\mathbf{H})\,dV = (\mu_s-\mu_f)\frac{1}{V}\int_{V_s}\mathbf{H}\,dV.$$

Since $\langle \mathbf{H}_s \rangle = \frac{1}{V_s} \int_{V_s} \mathbf{H}\, dV$ and $V_s/V = 1 - \varepsilon$, we obtain the following relations for $\langle \mathbf{B} \rangle$ and $\langle \mu \rangle$ respectively:

$$\langle \mathbf{B} \rangle = \mu_f \langle \mathbf{H} \rangle + (\mu_s - \mu_f)(1 - \varepsilon)\langle \mathbf{H}_s \rangle, \tag{9}$$

$$\langle \mu \rangle = \mu_f + (1 - \varepsilon)(\mu_s - \mu_f) \cdot \langle H_s \rangle / \langle H \rangle. \tag{10}$$

In the last expression we have replaced vectors $\langle \mathbf{H} \rangle$ and $\langle \mathbf{H}_s \rangle$ by scalars because $\langle \mu \rangle$ does not depend on magnetic field orientation in an isotropic medium.

Now we have two equations (7) and (10) to express the unknown quantities $\langle \mathbf{H}_s \rangle$, $\langle \mathbf{H}_f \rangle$ as functions of $\langle \mathbf{H} \rangle$. For linear magnetic materials (MR fluid and particles of porous bed), we obtain:

$$\langle \mathbf{H}_s \rangle = \frac{\langle \mu \rangle - \mu_f}{(1 - \varepsilon)(\mu_s - \mu_f)} \cdot \langle \mathbf{H} \rangle, \tag{11}$$

$$\langle \mathbf{H}_f \rangle = \frac{\mu_s - \langle \mu \rangle}{\varepsilon(\mu_s - \mu_f)} \cdot \langle \mathbf{H} \rangle. \tag{12}$$

The last step of the magnetic field calculation is the derivation of the effective magnetic permeability $\langle \mu \rangle$, which intervenes into Eqs. (8), (11), (12). There is a large amount of mean field theories (see [8,9]) for calculating the dielectric or magnetic constants of composite materials. We have to keep in mind that these mean field theories are not adapted for densely packed magnetic beds. They do not take into account the contacts of magnetic grains and closure of magnetic field lines on grains. Only numerical simulations are able to give accurate results. When magnetic properties of the different phases do not differ much, the effect of contacts between grains is not very important and, in practice, all the theories give a good agreement with simulation results [9] when $\mu_s/\mu_f < 4{-}5$. So, for non-magnetic porous beds used in our experiments, we shall use Maxwell–Garnett theory. This theory considers spherical grains dispersed randomly in a carrier medium and subjected to a local field, called Lorentz field [8]. Such representation of a porous medium seems to well represent the real situation of densely packed beds. For a bed of spherical grains it gives the following results for the effective permeability [8]:

$$\langle \mu \rangle = \frac{\mu_f(1 + 2(1 - \varepsilon)\beta)}{1 - (1 - \varepsilon)\beta}, \tag{13}$$

with $\beta = (\mu_s - \mu_f)/(\mu_s + 2\mu_f)$.

Inserting Eq. (13) into Eq. (12) reads:

$$\langle \mathbf{H}_f \rangle = \frac{1}{1 - (1 - \varepsilon)\beta} \cdot \langle \mathbf{H} \rangle, \tag{14}$$

Eq. (13) can be easily extended to the case of non-spherical grains. Since the majority of granular particles can be approximated by a triaxial ellipsoid, we have calculated $\langle \mu \rangle$ for a packed bed of ellipsoidal grains (see Appendix for details of derivation):

$$\langle \mu \rangle = \mu_f \cdot \left[1 + (1 - \varepsilon) \sum_{i=1}^{3} (1 - N_i)\beta_i \right] \Big/ \left[1 - (1 - \varepsilon) \sum_{i=1}^{3} N_i \beta_i \right], \tag{15}$$

where N_i $(i = 1, 2, 3)$ are demagnetization factors of an ellipsoid along its main axes, and $\beta_i = (1/3) \cdot (\mu_s - \mu_f)/(\mu_f + N_i(\mu_s - \mu_f))$.

For a bed of spherical grains, $N_i = 1/3$ $(i = 1, 2, 3)$, and Eq. (15) reduces to Eq. (13). For non-magnetic cylindrical particles (of length-to-diameter ratio l/d) used in experiments, we calculate demagnetization factors as for an ellipsoid of revolution with the same major-to-minor semi-axis ratio l/d. Values of N_i are given by formulas [7]: $N_1 = [(1 - e^2)/e^3][\operatorname{atanh}(e) - e]$ for $l/d > 1$, $N_1 = [(1 + e^2)/e^3](e - \operatorname{atan}(e))$ for $l/d < 1$, $N_2 = N_3 = (1 - N_1)/2$ with $e = |1 - 1/(l/d)^2|^{1/2}$ being the eccentricity of an ellipsoid.

For high ratios μ_s/μ_f most of the mean field theories fail but some of them give an unexpectedly good correspondence with the numerical result. For instance, Looyenga theory gives a very simple analytical expression for spherical particles with $\mu_p/\mu_f < 100$ [10]:

$$\langle \mu \rangle = \left[\varepsilon \mu_f^{1/3} + (1 - \varepsilon)\mu_s^{1/3} \right]^3. \tag{16}$$

Analyzing Eqs. (16) and (12), one can conclude that, if the solid phase has higher magnetic permeability than the liquid phase ($\mu_s > \mu_f$ case of MR fluid in a magnetic porous matrix), then the mean field $\langle H_f \rangle$ in the liquid phase exceeds the mean one $\langle H \rangle$. On the contrary, in non-magnetic matrix ($\mu_s < \mu_f$) the mean field $\langle H_f \rangle$ is always lower than $\langle H \rangle$. It supports our previous hypothesis (see Section 3) that the field $\langle H_f \rangle$ in magnetic porous bed exceeds the one in non-magnetic bed for the same external field H_0.

We shall use the formula (16) for calculation of magnetic fields in a packed bed of magnetic spheres, that we have used in experiment. Despite the simplicity of the result (16), its extension to the case of ellipsoidal grains seems to be quite difficult. Furthermore, we are not sure that this modification will give a correct result for such high ratios μ_s/μ_f. Thus, we restrict ourselves only to theoretical consideration of magnetic grains of spherical shape.

While calculating mean fields in beds of spherical magnetic grains, we take into account the magnetization law (1) of bulk steel. Since grains are packed inside a long cylindrical column subject to a longitudinal external field $\mathbf{H}_0$, demagnetization effect of the column is absent, so $\langle \mathbf{H} \rangle = \mathbf{H}_0$. First, as Eq. (1) applies to the solid phase we use the mean field $\langle H_s \rangle$ into Eq. (1) for obtaining $\mu_s(\langle H_s \rangle)$. Then we substitute the function $\mu_s(\langle H_s \rangle)$ into Eqs. (16) and (11) for $\langle \mu \rangle$ and $\langle \mathbf{H}_s \rangle$ respectively. Eq. (11) becomes therefore a transcendental equation for $\langle H_s \rangle$ that we solve numerically. So, for a given value $\langle H_s \rangle$ we obtain the corresponding value of $\mu_s(\langle H_s \rangle)$. Finally, substituting the result for $\mu_s(\langle H_s \rangle)$ into Eqs. (16) and (12), we obtain numerical results for $\langle \mu \rangle$ and $\langle \mathbf{H}_f \rangle$ respectively, versus the field $\langle H \rangle = H_0$.

The most important value obtained from this calculation is the factor $f_d = \langle H_f \rangle / H_0$ for each porous sample that is given in Table 1. For magnetic beds this factor is calculated for the external field $H_0 = 20\ \mathrm{kA \cdot m^{-1}}$.

4.2. Yield stress and pressure gradient

Let us consider the model of tortuous channels represented in Fig. 5. Magnetic field is assumed to be uniform inside the MR fluid and equal to the mean field $\langle \mathbf{H}_f \rangle$ in the liquid phase. For the sake of completeness, we shall study the general case where the direction of mean field $\langle \mathbf{H}_f \rangle$ (as well as of $\langle \mathbf{H} \rangle$) makes an angle $0 \leqslant \alpha \leqslant \pi$ with the mean flow direction (superficial velocity $\mathbf{v}_0$). Channels have all the same radius equal to the equivalent radius R_e of pores. One given channel can be represented by a broken line consisting of a large number, m, of rectilinear segments having the same length h. Segments are randomly oriented in space and their orientation is defined by the angles θ and ϕ with θ the angle between the velocity $\mathbf{v}_0$ and a segment of the channel, and ϕ the polar angle in the plane perpendicular to $\mathbf{v}_0$. The reference axis for ϕ is the magnetic field component $\langle \mathbf{H}_f \rangle_\perp$ normal to the velocity $\mathbf{v}_0$ (cf. Fig. 5(b)).

In isotropic medium any channel orientation is equivalent with respect to the polar angle ϕ and is described by the only frequency distribution function $\mathrm{f}(\theta)$. In order to determine this function, we take into account the following considerations.

1. Since the primary direction of the flow corresponds to the angle $\theta = 0$, and the less probable direction does to $\theta = \pi$, the frequency distribution function $\mathrm{f}(\theta)$ should take maximal and minimal values in points $\theta = 0$ and $\theta = \pi$ correspondingly.

2. For porous media formed by straight channels the only direction of the flow is $\theta = 0$, so the frequency distribution function should take the form

$$\mathrm{f}(\theta) = \begin{cases} \infty, & \theta = 0, \\ 0, & \theta \neq 0. \end{cases}$$

3. In a porous medium with infinite tortuosity, each direction of local flow has equal probability, so the function $\mathrm{f}(\theta)$ should be uniform:

$$\mathrm{f}(\theta) = \begin{cases} 1/2, & \theta \in [0, \pi], \\ 0, & \theta \notin [0, \pi]. \end{cases}$$

4. The number of unknown parameters of the function $\mathrm{f}(\theta)$ is two (λ_1 and λ_2). They are determined from the normalization condition and the expression for channel tortuosity. According to the model of tortuous channels, tortuosity is defined as

$$\xi = \frac{mh}{h \sum_{i=1}^{m} \cos(\theta_i)} = \frac{1}{\langle \cos(\theta) \rangle}. \tag{17}$$

Therefore the equations for determinig the parameters λ_1 and λ_2 takes the form:

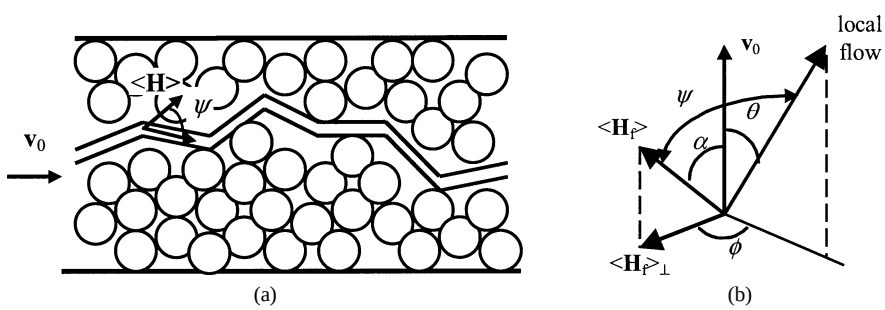

Fig. 5. (a) Model of a porous medium; (b) Sketch of the angle ψ between local flow and field in the MR fluid.

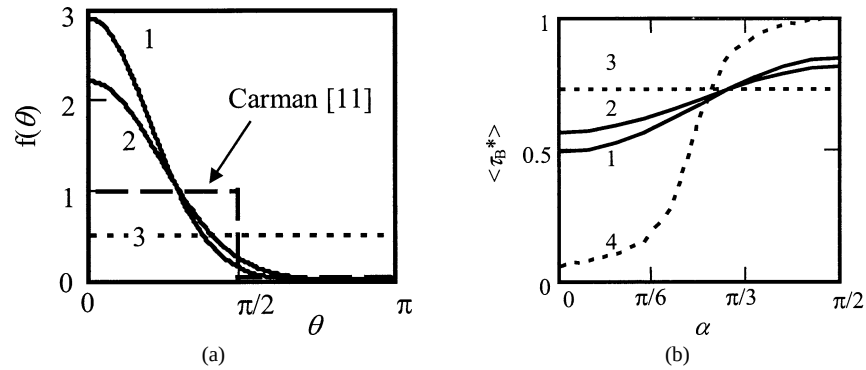

Fig. 6. (a) The distribution function $f(\theta)$ of channel orientations; (b) Dependence of the mean reduced yield stress of a MR fluid in porous media on the magnetic field orientation angle, α, relative to the mean flow direction. 1 – bed of spheres: $\xi = 1.44$, 2 – bed of cylinders: $\xi = 1.63$, 3 – channels of infinite tortuosity: $\xi \to \infty$, 4 – straight channels: $\xi = 1$.

$$\int_{-\infty}^{\infty} f(0)\sin(\theta)\,d\theta = 1, \tag{18}$$

$$\frac{1}{\int_0^{\pi} f(\theta)\cos(\theta)\sin(\theta)\,d\theta} = \xi. \tag{19}$$

In a classical work [11] the author postulates that all directions of local flows corresponding to $\theta \leqslant \pi/2$ in a packed bed of spheres are equal and that reverse flows ($\theta > \pi/2$) do not occur. Thus, the distribution function is

$$f(\theta) = \begin{cases} 1, & \theta \in [0, \pi/2], \\ 0, & \theta \notin [0, \pi/2]. \end{cases}$$

He calculates tortuosity using mean angle $\langle\theta\rangle = \pi/4$ between streamlines of local flows and mean flow: $\xi = 1/\cos\langle\theta\rangle = \sqrt{2}$. This result is in an excellent agreement with experiments, although the correct expression Eq. (17) for tortuosity gives $\xi = 2$.

We choose a Gauss like function $f(\theta)$, that keeps some resemblance with the shape of the step-function proposed in [11] (the curve marked 'Carman' in Fig. 6(a)) and satisfies all the requirements specified above:

$$f(\theta) = \begin{cases} 0, & \theta \notin [0, \pi], \\ \lambda_1 \exp(-\lambda_2 \theta^2), & \theta \in [0, \pi]. \end{cases} \tag{20}$$

The distribution function $f(\theta)$ is shown in Fig. 6(a). The peak value $f(0)$ is higher for the bed of spheres ($\xi = 1.44$, curve 1) compared to the bed of cylindrical grains ($\xi = 1.63$, curve 2). The probability of reverse local flows ($\theta > \pi/2$) is almost zero for both beds. The higher tortuosity, the closer is the distribution function to the uniform one $f(\theta) = 1/2$ applied to a porous medium of infinite tortuosity (curve 3).

As local values of τ_B and η_p on a given segment of a channel, we take those obtained experimentally for a long cylindrical channel [5]. Therefore τ_B and η_p are functions of the value and orientation ψ of the field $\langle \mathbf{H}_f \rangle$, where ψ is the angle between the channel axis line and magnetic field lines (cf. Fig. 5(b)). It can be expressed through known values θ, ϕ, α, if we consider the scalar production of two unite vectors $\mathbf{i}_C$ and $\mathbf{i}_H$ in the direction of the local flow and of the field correspondingly (Fig. 5(b)). The coordinates of these vectors are $(\sin(\theta)\cos(\phi),\ \sin(\theta)\sin(\phi),\ \cos(\theta))$ and $(\sin(\alpha),\ 0,\ \cos(\alpha))$, the angle between them is ψ. So, for $\cos(\psi)$ we obtain:

$$\cos(\psi) = \sin(\theta)\cos(\phi)\sin(\alpha) + \cos(\theta)\cos(\alpha). \tag{21}$$

The empirical dependence of the yield stress τ_B on the field $\langle H_f \rangle$ and angle ψ takes the form [5]:

$$\tau_B = \tau_{B0}\big(\langle H_f \rangle\big) \cdot \tau_B^*(\psi), \tag{22}$$

$$\tau_B^* = \begin{cases} q(\psi), & 0 \leqslant \psi \leqslant \dfrac{\pi}{2}, \\ q(\pi - \psi), & \dfrac{\pi}{2} < \psi \leqslant \pi, \end{cases} \qquad q(\psi) = 0.3353\,\mathrm{acot}\left[7.594\left(\frac{\pi}{2} - \psi\right) - 6.263\right]. \tag{23}$$

Here, the reduced yield stress $\tau_B^* = \tau_B/\tau_{B0}$ is the ratio of the yield stress for the given field orientation to that τ_{B0} for the transverse field ($\psi = \pi/2$). The empirical dependence $\tau_{B0}(\langle H_f \rangle)$ is given by Eq. (2). The symmetry of the function $\tau_B^*(\psi)$

relatively to $\psi = \pi/2$ corresponds to the equivalency of ψ and $\pi - \psi$ for the magnetic field orientation with respect to the velocity $\mathbf{v}_0$. There is no obvious dependence of the plastic viscosity on the magnitude and orientation of the field. In both experiments with single channel [5] and porous media (Section 3 of the present paper) η_p (or $\langle\eta_p\rangle$) does not varies significantly with the orientation of the magnetic field. Thus, we assume that η_p is constant over the whole volume V_f of MR fluid in a porous medium and equal to its value in the absence of the field.

The yield stress τ_B is averaged over the random orientation of a tortuous channel, i.e., over the solid angle 4π:

$$\langle\tau_B\rangle = \tau_{B0} \cdot \langle\tau_B^*\rangle, \tag{24}$$

$$\langle\tau_B^*\rangle = \frac{1}{2\pi}\int_0^{2\pi}\int_0^{\pi} f(\theta)\tau_B^*(\psi)\sin(\theta)\,d\theta\,d\phi. \tag{25}$$

The angle ψ is given by Eq. (21) and $\tau_B(\psi)$ by Eqs. (22), (23).

To demonstrate the orientation effect of the external magnetic field or, rather, the field $\langle\mathbf{H}\rangle$, on MR fluid flow in a porous medium, we plot the dependence of the mean yield stress $\langle\tau_B^*\rangle$ on the angle α between the field $\langle\mathbf{H}\rangle$ and the velocity $\mathbf{v}_0$ (Fig. 6(b)). The value of unity corresponds to straight channel in a perpendicular field. In this case, where the tortuosity is unity, the dependence on α is shown by the dotted curve (curve 4). When the tortuosity increases, the different orientations of the channels characterized by $f(\theta)$ contribute to smooth the angular dependence of the yield stress; nevertheless, there is still a factor of about 1.5 for the bed of cylinders (curve 2 with $\xi = 1.63$) between aligned field ($\alpha = 0$) and perpendicular field ($\alpha = \pi/2$). The absence of dependence is obtained for infinite tortuosity (curve 3) but with a value of 0.73 instead of unity for straight channels in perpendicular field. The case of a bed of spheres (curve 1) is quite close to the one of long cylinders.

For the external field longitudinal to the flow, as in our experiment, we have $\alpha = 0$, so $\psi = \theta$, and the expression (25) reduces to

$$\langle\tau_B^*\rangle = \int_0^{\pi} f(\theta)\tau_B^*(\theta)\sin(\theta)\,d\theta. \tag{26}$$

In a general way we can conclude that the higher the tortuosity of a porous medium, the narrower the range of mean yield stress variation.

To calculate the pressure gradient, we should substitute the mean yield stress given by Eqs. (24), (25) into Eq. (6). In order to obtain $\Delta P/L$ as a function of the external magnetic field H_0, we should express the field H_f intervening in τ_{B0}: $\tau_{B0} = 10\mu_0 H_f^2 = 10\mu_0 f_d^2 H_0^2$. The calculation of factor $f_d = \langle H_f\rangle/H_0$ has been described in Section 4.1. For long columns of porous beds subjected to the longitudinal field, $\langle H\rangle = H_0$, f_d is determined either with Eqs. (12), (15) for non-magnetic grains or with Eqs. (12), (16) for magnetic ones. For the bundle of long cylinders $f_d = 1$. Finally, we obtain the following formula for the mean yield pressure gradient $(\Delta P/L)_{v=0}$:

$$\left(\frac{\Delta P}{L}\right)_{v=0} = \frac{16\xi}{3\pi R_e} \cdot 10\mu_0 f_d^2 H_0^2 \cdot \langle\tau_B^*\rangle. \tag{27}$$

We have compared in Fig. 7 the experimental values of $(\Delta P/L)_{v=0}$ to the theoretical predictions given by Eq. (27). The theory, represented by the solid curve, is quite close to the experimental results. The slight difference for cylinders could come

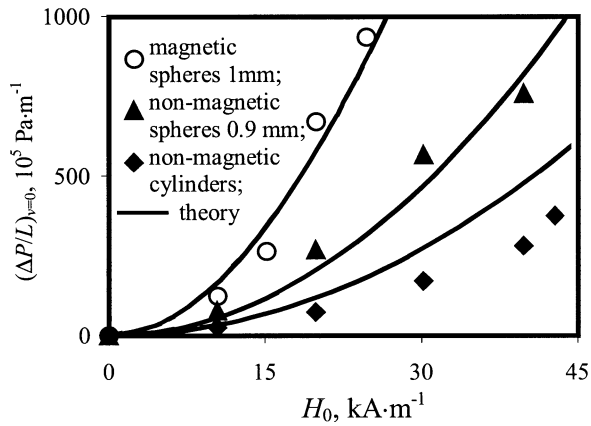

Fig. 7. Dependence of the yield pressure gradient in different porous beds on the external magnetic field H_0; comparison theory-experiment.

from the channel distribution function f(θ) that, for cylinders, likely underpredicts the number of channels aligned with the main axis of flow.

5. Conclusions

We have given new experimental results concerning the flow of a MR fluid through different kinds of porous media. A model aiming to predict the pressure drop versus magnetic field in porous media has been presented, that well reproduces our experimental results. This model emphasizes the role of tortuosity on the increase of pressure drop, through the dependence of yield stress on the angle between field and flow. It also shows that a packed bed of magnetic grains gives a much higher pressure drop than a bed of non-magnetic grains. Using this model we are able to compare the efficiency of various kinds of porous beds and spiral channels for the control of pressure drop with a MR fluid. This will be the subject of a future work.

Acknowledgements

This work is supported by the European association INTAS and the Belarussian Foundation of Fundamental Researches. We are very grateful to A. Audoly and J. Blanchard for fabrication and maintenance of the experimental equipment and to C. Laye for MR fluid preparation.

Appendix A. Calculation of the effective magnetic permeability of a packed bed of ellipsoidal grains

In order to determine $\langle\mu\rangle$ we need to know the mean field $\langle H_s\rangle$ in the solid phase (see Eq. (10)). First we calculate the magnetic field $\mathbf{H}_s$ inside an arbitrary ellipsoidal grain. According to Maxwell Garnett, each grain is immersed into a medium with permeability μ_f and an external field $\mathbf{H}^L$ called the Lorenz field [8]. Thus, the field $\mathbf{H}_s$ inside a grain is determined by the following expression:

$$\mu_f\mathbf{H}_s + (\mu_s - \mu_f)\mathbf{N}\cdot\mathbf{H}_s = \mu_f\mathbf{H}^L, \tag{A.1}$$

where $\mathbf{N}$ is the tensor of demagnetization factors of an ellipsoidal grain. The Lorenz field for spherical particles is given by the formula [8] $\mathbf{H}^L = (2\mu_f + \langle\mu\rangle)\langle\mathbf{H}\rangle/(3\mu_f)$, that can be extended to the general case of ellipsoidal particles:

$$\mathbf{H}^L = \left(\frac{1}{\mu_f}\right)\cdot\left[\mu_f\langle\mathbf{H}\rangle + \left(\langle\mu\rangle - \mu_f\right)\mathbf{N}\cdot\langle\mathbf{H}\rangle\right]. \tag{A.2}$$

We choose a Cartesian coordinate system (x, y, z) in such a way that the axis z coincides with the direction of the magnetic field $\langle\mathbf{H}\rangle$. The second Cartesian coordinate system (x', y', z') is adjusted to the axes of an ellipsoidal grain. The system (x', y', z') is formed from the original one (x, y, z) by rotation of an angle θ about the axis y followed by a rotation of angle ϕ around axis z'. The rotation matrix of these transformations takes the form [12]:

$$\boldsymbol{\Omega} = \begin{pmatrix} \cos(\theta)\cos(\phi) & -\sin(\phi) & \sin(\theta)\cos(\phi) \\ \cos(\theta)\sin(\phi) & \cos(\phi) & \sin(\theta)\sin(\phi) \\ -\sin(\theta) & 0 & \cos(\theta) \end{pmatrix}. \tag{A.3}$$

Projections of the magnetic field $\langle\mathbf{H}\rangle$ on coordinate axes x', y' and z' of a grain are determined from the following matrix relation: $\langle\mathbf{H}'\rangle = \boldsymbol{\Omega}\cdot\langle\mathbf{H}\rangle$. Hereinafter all vector and scalar magnitudes considered in the coordinate system (x', y', z') are denoted by a stroke. Projections of the magnetic field $\mathbf{H}_s$ on axes x', y' and z' are calculated from Eqs. (A.1), (A.2):

$$H'_{si} = a_i\cdot\langle H'\rangle_i, \tag{A.4}$$

with $a_i = [\mu_f + N_i(\langle\mu\rangle - \mu_f)]/[\mu_f + N_i(\mu_s - \mu_f)]$ and N_i $(i = 1, 2, 3)$ being demagnetization factors of an ellipsoidal particle in directions of particle axes.

Components $(H'_s)_i$ of the field $\mathbf{H}'_s$ are transformed into the original coordinate system (x, y, z) using the following relation: $\mathbf{H}_s = \boldsymbol{\Omega}^{-1}\cdot\mathbf{H}'_s$. So, we obtain the following expressions for the components of the field $\mathbf{H}_s$ inside a grain:

$$\begin{aligned} H_{sx} &= \left[a_1\cos(\theta)\sin(\theta)\cos^2(\phi) + a_2\cos(\theta)\sin(\theta)\sin^2(\phi) - a_3\cos(\theta)\sin(\theta)\right]\cdot\langle H\rangle, \\ H_{sy} &= \left[-a_1\sin(\theta)\sin(\phi)\cos(\phi) + a_2\sin(\theta)\sin(\phi)\cos(\phi)\right]\cdot\langle H\rangle, \\ H_{sz} &= \left[a_1\sin^2(\theta)\cos^2(\phi) + a_2\sin^2(\theta)\sin^2(\phi) + a_3\cos^2(\theta)\right]\cdot\langle H\rangle. \end{aligned} \tag{A.5}$$

Now we perform the averaging of components H_{si} over the solid angle 4π using the following relation: $\langle H_{si}\rangle = \frac{1}{4\pi}\int_0^{2\pi} \mathrm{d}\phi \int_0^{\pi} H_{si}\sin(\theta)\,\mathrm{d}\theta$. As expected, we obtain zero x- and y-components of $\langle \mathbf{H}_s\rangle$ and non-zero z-component. The final result for the mean field $\langle \mathbf{H}_s\rangle$ is:

$$\langle \mathbf{H}_s\rangle = \left[\frac{a_1 + a_2 + a_3}{3}\right] \cdot \langle \mathbf{H}\rangle = \langle a\rangle \cdot \langle \mathbf{H}\rangle. \tag{A.6}$$

Note that the relation [8] $\langle \mathbf{m}\rangle = \langle \alpha\rangle \cdot \mathbf{E}$ between the mean dipole moment $\langle \mathbf{m}\rangle$ of randomly oriented ellipsoidal particle and the external electric field $\mathbf{E}$ is similar to (A.6), i.e., the proportionality factor (polarizability α) is the arithmetic mean of its values for the main axes of the ellipsoid. Substituting $\langle \mathbf{H}_s\rangle$ from Eq. (A.6) into Eq. (10), we obtain a linear equation on $\langle \mu\rangle$ that we can solve (see Eq. (15)).

References

[1] Z.P. Shulman, W.I. Kordonsky, Magnetorheological Effect, Nauka i Tehnika, Minsk, 1982 (in Russian).
[2] Magnetic Fluids and Applications Handbook, B. Berkovski, V. Bashtovoi (Eds.), Begell House, New York, 1991.
[3] T.G. Savins, Nonlinear flow in porous media, Ind. Eng. Chem. 61 (1969) 18–47.
[4] N.-E. Sabiri, J. Comiti, Pressure drop in non-Newtonian purely viscous fluid flow through porous media, Chem. Engrg. Sci. 50 (1995) 1193–1201.
[5] P. Kuzhir, G. Bossis, V. Bashtovoi, O. Volkova, Effect of the orientation of the magnetic field on the flow of magnetorheological fluid. II. Cylindrical channel, submitted.
[6] N.G. Taktarov, Magnetizable fluid flow in porous media, Magmit. Gidrodinamika 16 (1980) 38–42.
[7] L.D. Landau, E.M. Lifchitz, Electrodynamics of Continuous Media, Nauka, Moscow, 1982 (in Russian).
[8] S. Berthier, Optique des milieux composites, Polytechnica, Paris, 1993.
[9] J. Widjajakusuma, B. Biswal, R. Hilter, Quantitative comparison of mean field mixing laws for conductivity and dielectric constants of porous media, Physica A 318 (2003) 319–333.
[10] H. Looyenga, Dielectric constants of heterogeneous mixtures, Physica 31 (1965) 401–406.
[11] P.C. Carman, Flow of Gases Through Porous Media, Butterworth, London, 1956.
[12] G.A. Korn, T.M. Korn, Mathematical Handbook for Scientists and Engineers, McGraw-Hill, New York, 1961.